



Predicting abundance and variability of ice nucleating particles in precipitation at the high-altitude observatory Jungfraujoch

Emiliano Stopelli¹, Franz Conen¹, Cindy E. Morris², Erik Herrmann³, Stephan Henne⁴, Martin Steinbacher⁴, and Christine Alewell¹

¹Environmental Geosciences, University of Basel, 4056 Basel, Switzerland

²INRA, UR 0407 Plant Pathology Research Unit, 84143 Montfavet, France

³PSI, Laboratory of Atmospheric Chemistry, 5232 Villigen, Switzerland

⁴Empa, Laboratory for Air Pollution/Environmental Technology, 8600 Dübendorf, Switzerland

Correspondence to: Emiliano Stopelli (emiliano.stopelli@unibas.ch)

Received: 2 February 2016 – Published in Atmos. Chem. Phys. Discuss.: 8 February 2016

Revised: 2 June 2016 – Accepted: 21 June 2016 – Published: 11 July 2016

Abstract. Nucleation of ice affects the properties of clouds and the formation of precipitation. Quantitative data on how ice nucleating particles (INPs) determine the distribution, occurrence and intensity of precipitation are still scarce. INPs active at -8°C (INPs₋₈) were observed for 2 years in precipitation samples at the High-Altitude Research Station Jungfraujoch (Switzerland) at 3580 m a.s.l. Several environmental parameters were scanned for their capability to predict the observed abundance and variability of INPs₋₈. Those singularly presenting the best correlations with observed number of INPs₋₈ (residual fraction of water vapour, wind speed, air temperature, number of particles with diameter larger than $0.5\ \mu\text{m}$, season, and source region of particles) were implemented as potential predictor variables in statistical multiple linear regression models. These models were calibrated with 84 precipitation samples collected during the first year of observations; their predictive power was successively validated on the set of 15 precipitation samples collected during the second year. The model performing best in calibration and validation explains more than 75 % of the whole variability of INPs₋₈ in precipitation and indicates that a high abundance of INPs₋₈ is to be expected whenever high wind speed coincides with air masses having experienced little or no precipitation prior to sampling. Such conditions occur during frontal passages, often accompanied by precipitation. Therefore, the circumstances when INPs₋₈ could be sufficiently abundant to initiate the ice phase in clouds may frequently coincide with meteorological conditions favourable to the onset of precipitation events.

1 Introduction

Ice nucleating particles (INPs) play an essential role in the formation of precipitation on Earth, specifically on the continents, where most precipitation comes from ice- or mixed-phase clouds (Mülmenstädt et al., 2015). INPs catalyse the first aggregation of water molecules into ice crystals, which progressively grow larger by diffusion of surrounding water vapour and by collision with water droplets and other ice crystals until they reach a sufficient size to precipitate. In the absence of INPs, spontaneous freezing would occur only at temperatures below -36°C (Cantrell and Heymsfield, 2005; Murray et al., 2012).

The scarcity of data about the atmospheric abundance and distribution of INPs prevents a quantitative assessment of their effect on cloud properties, on the development of precipitation and subsequently on climate. Several studies have shown the co-occurrence of INPs from local or far-away sources with precipitation at sites in the Amazon forest (Pöschl et al., 2009; Prenni et al., 2009), in the Sierra Nevada region (Creamean et al., 2013), and at a forested site in Colorado (Huffman et al., 2013; Prenni et al., 2013). The prediction of atmospheric concentrations of INPs from more easily accessible parameters would allow for a more thorough evaluation of the influence of INPs on clouds and precipitation. This approach merits attention in light of results showing the correlation of specific meteorological and environmental parameters with the abundance of INPs, such as air temperature (Conen et al., 2015), wind speed (Jiang et al., 2014; Jones

and Harrison, 2004), relative humidity (Bowers et al., 2009; Wright et al. 2014), season and geographical source (Christner et al., 2008), and the abundance of airborne particles of micrometre size (DeMott et al., 2010). In addition, we have recently shown that the abundance of INPs active at moderate supercooling negatively correlates with the amount of water that has been lost from an air mass prior to sampling (Stopelli et al., 2015). All these studies indicate statistical relations between INPs and the mentioned parameters, but each tends to focus predominantly on the role of a single parameter.

Here our objective is to describe and foresee the variations in the concentration of INPs active at -8°C or warmer (INPs₋₈) in falling precipitation at the high-altitude observatory Jungfraujoch (Swiss Alps, 3580 m a.s.l.) by means of multiple linear regression models. INPs₋₈ are of particular interest since it has been proposed that the ice phase in clouds could be initiated by relatively few INPs₋₈ (10 m^{-3} or less) through the Hallet–Mossop process of riming and ice splintering (Crawford et al., 2012; Mason, 1996). To attain our objective, we firstly identified the strongest predictors for the abundance of INPs₋₈ in precipitation among all the environmental parameters measured at the observatory. Secondly, we implemented these predictors in three multiple linear regression models built on the temporal variations in INPs₋₈ occurred during the first year of observations ($n = 84$). The predictive power of these statistical models was subsequently tested on an independent set of samples from the second year of measurements ($n = 15$). Prediction of the quantity of INPs₋₈ provides useful means to understand the factors responsible for their large variability in precipitation (Petters and Wright, 2015) and to indicate the circumstances when and where INPs₋₈ may be sufficiently abundant to impact the formation of the ice phase in clouds and conduce to precipitation.

2 Methods

2.1 Sample collection and analysis of INPs

Falling snow was collected at the High Altitude Research Station Jungfraujoch in the Swiss Alps ($7^{\circ}59'06''\text{E}$, $46^{\circ}32'51''\text{N}$; 3580 m a.s.l.) from December 2012 until October 2014. A total of 106 precipitation samples were collected over these 2 years, with a median sampling duration of about 2 h per sample (sampling time between 1.5 and 8 h), depending on the intensity of the precipitation events. We started sampling campaigns when the forecasts predicted 2 or more days of precipitation to assure the collection of several samples during each campaign. Samples were collected with a Teflon-coated tin carefully rinsed with ethanol and sterile Milli-Q water to avoid cross-contamination.

Snow samples were analysed for the concentrations of INPs₋₈ directly on site, using the automated drop freeze apparatus LINDA (LED-based Ice Nucleation Detection Appa-

ratus) loaded with 52 tubes containing 100 μL of sample each (prepared adding 2 mL of 9 % NaCl sterile solution to 18 mL of sample and gently shaken, to ensure a final physiological saline concentration and improve the detection of freezing events, dilution 1 : 1.1; Stopelli et al., 2014, 2015). Blanks were periodically prepared distributing sterile Milli-Q water onto the rinsed tin and analysed with the same procedure as the snow samples, with 200 μL per tube to obtain more restrictive results. Out of 29 blanks analysed during the sampling campaigns reported here, only two blanks contained 0.11 INPs₋₈ mL^{-1} , confirming the accuracy of our analyses.

Error bars for values of 1, 10, 100, and 1000 INPs₋₈ mL^{-1} are shown in the figures of the article. Confidence intervals were calculated as errors in counting frozen tubes, following Poisson's distribution (depending on the number of frozen tubes, they account for 30 to 50 % increase or decrease of the calculated concentrations of INPs₋₈). These intervals were propagated into the uncertainty associated with the maximum error in the determination of the freezing temperature of the tubes of $\pm 0.2^{\circ}\text{C}$ (assuming a doubling of INPs per $^{\circ}\text{C}$ of decrease in the freezing temperature, an error of 0.2°C accounts for a change in 14 % of the measured concentrations) to provide more cautious confidence intervals.

The collection of precipitation allows for the sampling of INPs that either formed precipitating ice particles or were scavenged by precipitation. It is difficult to distinguish between these contributions in field studies, where scavenging, riming, and crystal growth by vapour deposition can alter the abundance of INPs in precipitation. Nevertheless, the station was always inside clouds while sampling, allowing us to collect falling snow as close as possible to where it formed. Furthermore, precipitation was immediately analysed, in order to minimise the chance for biases due to artefacts like the production (i.e. the release in solution of INPs or cellular multiplication) and the loss (i.e. settling or increased molecular weakness of biological INPs detached from mineral and soil dust) of INPs₋₈.

2.2 Parameters related to the concentration of INPs

To analyse and understand more on the factors responsible for the variability of INPs₋₈ in precipitation, several environmental parameters were considered in relation with the number of INPs₋₈.

INPs are efficiently removed by precipitating clouds (Stopelli et al., 2015). Therefore, important information on the residual abundance of INPs in rain and snow samples is contained in the value of the residual fraction of water vapour in the sampled air mass f_V . Water molecules containing the stable isotope ^{18}O have a greater propensity to condense, hence to precipitate, than those containing the more abundant stable isotope ^{16}O . Consequently, the $^{18}\text{O} : ^{16}\text{O}$ ratio (indicated as δ) in an air mass decreases during precipitation. f_V can be easily calculated comparing the isotopic ratio of the initial water vapour content of an air mass at the moment of

its formation with the ratio at the moment of sampling according to Rayleigh's fractionation model (IAEA, 2001):

$$\frac{\delta_V}{1000} = \left(1 + \frac{\delta_{V,0}}{1000}\right) \cdot f_V^{\alpha_{LV}-1} - 1. \quad (1)$$

In this study δ_V is the isotopic ratio of the vapour at Jungfraujoch, calculated from the isotopic ratio of sampled snow, $\delta_{V,0}$ is the modelled isotopic ratio of the vapour in an air mass at the moment of its formation in contact with seawater and α_{LV} is the fractionation factor from liquid to water along the trajectory of a cloud. Further details on the calculation of these parameters are presented in Stopelli et al. (2015).

Wind speed, air temperature, and relative humidity are continuously measured at Jungfraujoch by MeteoSwiss and are stored as 10 min averages. An optical particle counter (GrimmTM, Dust Monitor 1.108) mounted in series with a heated inlet regularly measures the total number of particles with a dry optical diameter larger than $0.5 \mu\text{m}$ ($N_{>0.5}$) (Weingartner et al., 1999; WMO/GAW, 2003). To produce robust statistics, it was important to assign a single value of air temperature, wind speed and $N_{>0.5}$ to each snow sample. These parameters had a finer temporal resolution compared to the measurements of INPs₈; therefore, they were averaged over the time interval during which each snow sample was collected. To fill gaps due to instrument failures, missing $N_{>0.5}$ values (26 out of 106 samples) were estimated by linear regression from measured PM₁₀ concentrations ($R^2 = 0.40$, $p < 0.001$), which are continuously determined at Jungfraujoch by Empa (the Swiss Federal Laboratories for Materials Science and Technology) through a beta-attenuation method (Thermo ESM Andersen FH62 IR). Due to the usually low PM₁₀ concentrations at Jungfraujoch, data are aggregated to hourly averages to achieve better signal to noise ratios. In this case, the PM₁₀ concentration corresponding to each snow sample was calculated averaging the hourly values including the whole duration of the collection of the sample. Empa also provided hourly concentrations of CO and total reactive nitrogen NO_y in the air. The ratio NO_y / CO is a common proxy of the age of an air mass; thus, it was used as indicator of planetary boundary layer influence and recent land contact of air masses sampled at the observatory (Griffiths et al., 2014; Pandey Deolal et al., 2013). Due to different susceptibility to photochemical transformation in the atmosphere, NO_y / CO ratios decrease during transport after being emitted from anthropogenic sources. Therefore, a larger ratio of NO_y / CO is associated with a more recent contact of the air masses with land surface. Threshold values in the range 0.002 to 0.008 have been proposed to distinguish between conditions influenced by planetary boundary layer and free tropospheric air masses (Fröhlich et al., 2015; Pandey Deolal et al., 2013).

Precipitation intensity (mm h^{-1}) was calculated by dividing the water-equivalent volume of precipitation collected in the sampling tin by its horizontal surface and the sampling duration.

Potential regions where air masses could have picked up particles on their way to Jungfraujoch were determined by the analysis of source sensitivities simulated with FLEXPART, a Lagrangian particle dispersion model used in backward mode (Stohl et al., 2005). FLEXPART was driven with analysed meteorological fields taken from the ECMWF integrated forecasting systems with a horizontal resolution of 0.2° by 0.2° over the Alpine area and 1° by 1° elsewhere (more details on the specific set-up for Jungfraujoch simulations can be found in Brunner et al., 2013). A "source region score" was assigned to each sample, combining information derived from the visual inspection of potential source regions in FLEXPART plots with the prevailing wind direction during sampling. This categorical parameter was conceived to mirror the potential differences in source quality and source strength of INP populations between northern and southern Europe. Three groups were identified: north, south, and mixed/uncertain conditions. A priori it was hypothesised that a higher score should be given to samples from southern Europe, assuming a larger influence of warmer air masses, enriched in larger mineral dust and organic material emissions, also linked to a more prolonged duration of agricultural activities (Kellogg and Griffin, 2006; Lindemann et al., 1982; Morris et al., 2014). Therefore, a priori the larger value should be assigned to events from south, followed by mixed conditions and by events from northern Europe. Several combinations of values ranging from 1 to 3 (2–1.5–1, 3–2–1, etc.) were tested and the best combination of values was determined through comparisons with the numbers of $\log(\text{INPs}_{8} \text{ mL}^{-1})$. It corresponds to the following: south is for 3, mixed condition for 2, and north for 1.

A similar approach was used to insert the "season score", a categorical parameter mirroring the potential effects of seasonality on the release and abundances of INPs₈. A priori the highest value was assigned to samples collected in summer, assuming both a larger release of soil and organic material containing INPs, associated with the growth of vegetation, agricultural activity, and warmer air masses (Jones and Harrison, 2004; Lindow et al., 1978; Morris et al., 2014) and a greater chance for INPs to reach the observatory before being removed by precipitation (Conen et al., 2015). In the ranking, summer was followed by autumn and spring as intermediate seasons, and finally by winter. Once this a priori classification was established, the precise values for each class were again determined by comparing different possible combinations of numbers from 1 to 9 (3–2–2–1, 9–6–3–1, 4–3–2–1, etc.) with measured values of $\log(\text{INPs}_{8} \text{ mL}^{-1})$. The best fit with the data was found for the combination: summer is for 4; autumn for 3; spring for 2; winter for 1.

2.3 Statistical analyses and modelling

Univariate statistics were carried out with PAST software version 2.17. The R software version 3.0.1 was used to build

multiple linear regression models (Hammer et al., 2001; R Core Team, 2011).

The first step in model building consisted of a preliminary screening of the environmental parameters that had a significant relation with the variability in INPs₋₈. This was done considering both the results of parametric linear regression and Spearman's non-parametric correlation test. For the categorical parameters "season score" and "source region score" the results of parametric regression were conservatively substituted with Kruskal–Wallis non-parametric test for the comparison among groups, because this test takes into account the presence of different numbers of data among groups. Normal distribution of variables is required for parametric statistics. In particular, the concentrations of INPs₋₈ were approximately log-normally distributed over several orders of magnitude. Therefore, they were log₁₀ transformed to normalise their distribution. This led to the exclusion of 7 of 106 samples with no measurable activity (< 0.21 INPs₋₈ mL⁻¹): the arbitrary assignment of small concentrations would have resulted in a bias when projected on the log scale. Similarly, the number of particles $N_{>0.5}$, precipitation intensity and the ratio NO_y / CO were log₁₀ transformed to improve the distribution of their data. Non-parametric correlation was added to draw more robust and stricter conclusions, independent from parameter distributions.

Multiple linear regression models were built on the parameters presenting the best correlations with INPs₋₈. Criteria to build up the models were (a) to start from the addition of two parameters, which we a priori suspected could be descriptors of environmental processes impacting INPs₋₈ in different ways, such as proxies for their production and removal; (b) to add further parameters only if resulting in a significant gain in explained variability and improved distribution of the residuals; and (c) to prefer combinations of parameters weakly correlated among themselves (Table 1), to avoid collinearity.

The normal distribution of independent and dependent variables is considered as not necessary for assessing the quality of multiple linear regression models, but it can improve the quality of the results of the model. Consequently, the variables, which were log transformed for univariate statistics, were kept transformed also in multiple linear models. The quality of a multiple linear regression model is evaluated by the significance of the whole model as well as of the regression coefficients of each parameter. Particular care was taken in analysing the residuals of the models. All the models presented here fulfilled the conditions of normally distributed residuals, with an average value of zero and no significant trends. Furthermore, we assumed that the parameters could be added in linear combinations. The correctness of this assumption was verified by the method of partial regression plots of the residuals. Given an ideal model $y \sim x_1 + x_2$ (x_1 and x_2 used to derive the dependent variable y) it is possible to test whether i.e. x_2 is linearly linked to y . To do that, the residuals of the regression of y with x_2 are plotted against

the residuals of the regression of x_1 with x_2 . A linear distribution of the residuals confirms the correctness of the linear relationship between x_2 and y . On the contrary, the presence of a different trend implies a different relationship between x_2 and y , like, for example, a quadratic one. Interactions between independent variables were tested as well as potential ways to improve the models. This means that the additional factor $x_1 \cdot x_2$ was inserted in a model to test whether the effect of the independent variable x_1 (or x_2) on the dependent variable y changes according to different levels of the other independent variable x_2 (or x_1). No interaction we tested resulted in a significant improvement of the models.

3 Results and discussion

3.1 Model calibration

The observations used to create the models consist of 84 snow samples with measurable concentrations of INPs₋₈ collected in the Swiss Alps at 3580 m altitude between December 2012 and September 2013. Measured values of INPs₋₈ ranged from the lower limit of detection (0.21 mL⁻¹) to a maximum of 434 mL⁻¹. Interestingly, these values are comparable to, or even greater than those recently found in cloud water samples in central France at 1465 m altitude (Joly et al., 2014) and well within the range of values and variability observed in precipitation samples collected all around the world (Petters and Wright, 2015).

The best correlations found at Jungfraujoch agree with our current understanding of the factors that are related to the abundance of INPs in the environment (Fig. 1, black dots). In particular, the relationships with the remaining fraction of water vapour f_v and air temperature are coherent with the observation that INPs are rapidly lost by precipitating clouds; hence, they are more abundant at early stages of precipitation (Stopelli et al., 2015) and that colder air masses tend to be more depleted in INPs₋₈ (Conen et al., 2015). A better linear fit suggests that f_v is a factor capable of better representing the temporal variability in INPs₋₈ than air temperature, which shows a threshold trend. Specifically, it is possible to find more than 10 INPs₋₈ mL⁻¹ in precipitation for temperatures around 0 °C, indicating that when at the station the temperature is warm then also the temperature of precipitation formation in clouds above the Station can be compatible with residual large abundance of INPs₋₈, but not exclusively associated only to large values of INPs₋₈. Therefore, whilst air temperature appears more like a local snapshot-value for the potential activation of INPs₋₈, f_v is a broader descriptor of the cumulative precipitation history of an air mass.

Wind speed is a good proxy of the energy and turbulence associated with an air mass, promoting the transport and mixing of airborne particles (Jiang et al., 2014; Jones and Harrison, 2004). This is confirmed by the correlation between wind speed and log($N_{>0.5}$ m⁻³) (Table 1). Wind speed is

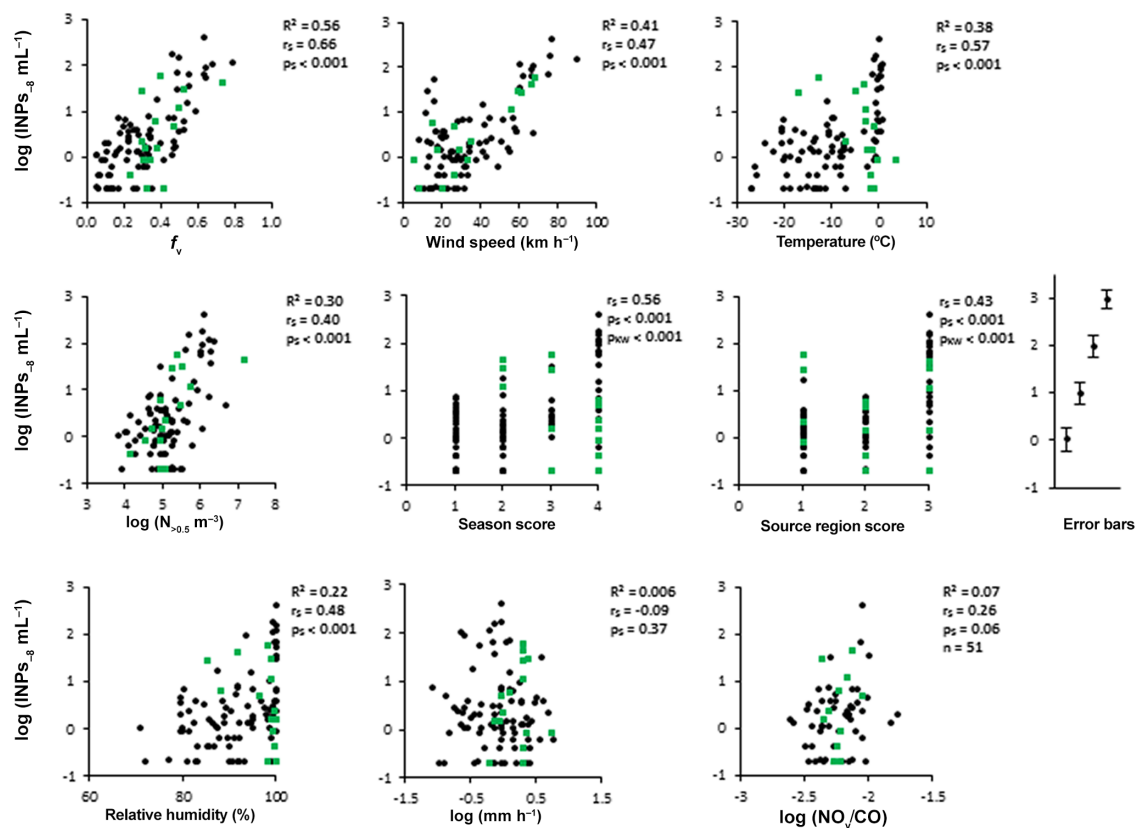


Figure 1. Relationships between $\text{INPs}_{-8} \text{ mL}^{-1}$ and singular environmental parameters for the first year of observations (black dots, $n = 84$, exception for the ratio NO_y / CO with $n = 51$ due to missing data of trace gases). Shown are R^2 values, the coefficient of Spearman's correlation r_s and its probability p_s calculated for the data belonging to the first year of observations. f_v indicates the remaining fraction of water vapour in a precipitating air mass. In the panel “season score” 1 is for winter, 2 for spring, 3 for autumn, and 4 for summer. In the panel “source region score” 1 is for northern Europe, 2 for mixed conditions and 3 for southern Europe. For both “season score” and “source region”, values of Kruskal–Wallis’ test probability p_{KW} are shown instead of R^2 . Data belonging to the second year of observations are represented as green squares ($n = 15$, $n = 12$ for the ratio NO_y / CO). Error bars associated to the measurement of 1, 10, 100, and 1000 $\text{INPs}_{-8} \text{ mL}^{-1}$ are represented close to the graphs.

not correlated to the direction of air masses, expressed by the source region score, indicating that the local morphology plays a minor role regarding this parameter. Coherently, the correlation between INPs_{-8} and $N_{>0.5}$ suggests that the more particles $N_{>0.5}$ are present in the air, the greater is also the probability of finding a greater abundance of INPs_{-8} . This relationship proved significant for INPs active at -15°C or colder (DeMott et al., 2010). Here we show its validity for INPs active at -8°C measured in precipitation at Jungfraujoch.

INPs_{-8} found in precipitation confirmed the expectations to be more abundant in summer and in air masses coming from southern Europe. Relative humidity appears as a threshold for the abundance of INPs_{-8} (Bowers et al., 2009; Wright et al., 2014), with a similar distribution of the data to the one shown by temperature. Therefore, the relationship between the relative humidity and INPs_{-8} may reflect the role of particle processing in the residual abundance of INPs_{-8} .

This process can be better represented by temperature or f_v ; thus, preference was given to the latter parameters in building multiple linear regression models. INPs_{-8} are not correlated with the intensity of precipitation, suggesting that different amounts of precipitation can be generated per INP. The ratio NO_y / CO presents a relatively low and homogeneous range of values, which are related to air masses with slightly recent contact with land surfaces (the most recent threshold value presented in literature for Jungfraujoch is 0.004, -2.4 on log scale; Fröhlich et al., 2015). Nevertheless, the sampling happened always inside precipitating clouds, which suggested the occurrence of the uplift of planetary boundary layer air to the height of the station. Therefore, it is realistic to speculate that the precipitation collected was generally originating from air masses integrating several source regions and distances before reaching the observatory. Furthermore, the ratio NO_y / CO is positively correlated with wind speed and $N_{>0.5}$ (Table 1), suggesting that at high wind speed clouds

Table 1. Pairwise correlations among predictors for the concentrations of INPs₋₈. The upper panel indicates the pairwise Spearman's r_s correlation coefficient, the lower panel its statistical significance (*, **, and *** stand for a probability smaller than 0.05, 0.01, and 0.001 respectively).

	f_V	Wind speed	Temperature	$\log(N_{>0.5} \text{ m}^{-3})$	Season	Source region	Relative humidity	$\log(\text{mm h}^{-1})$	$\log(\text{NO}_y / \text{CO})$
f_V		0.10	0.88	0.33	0.89	0.42	0.72	0.07	0.13
Wind speed			0.02	0.21	-0.04	0.17	0.04	0.08	0.31
Temperature	***			0.18	0.85	0.58	0.70	-0.03	-0.28
$\log(N_{>0.5} \text{ m}^{-3})$	**	*	*		0.35	0.32	0.28	-0.11	0.37
Season	***		***	***		0.38	0.77	-0.04	0.15
Source region	***		***	**	***		0.42	-0.12	-0.23
Relative humidity	***		***	**	***	***		-0.12	0.23
$\log(\text{mm h}^{-1})$		*	*	**		*	*		0.24
$\log(\text{NO}_y / \text{CO})$				**				*	

at Jungfraujoch may be charged with particles taken up during recent contact of the air mass with a land surface. This suggestion could explain larger numbers of INPs₋₈ in precipitation at high NO_y / CO ratios (Fig. 1).

The parameters presenting the best correlations with INPs₋₈ were successively added into multivariate linear regression models and the three models predicting the concentrations of INPs₋₈ best are

$$\log(\text{INPs}_{-8} \text{ mL}^{-1}) =$$

1. $2.84 \cdot f_V + 0.02 \cdot \text{wind speed}(\text{km h}^{-1}) - 1.12$
2. $0.36 \cdot \text{season} + 0.02 \cdot \text{wind speed}(\text{km h}^{-1}) + 0.13 \cdot \text{source region} - 1.39$
3. $0.02 \cdot \text{wind speed}(\text{km h}^{-1}) + 0.05 \cdot \text{temperature}(\text{°C}) + 0.34 \cdot \log(N_{>0.5} \text{ m}^{-3}) - 1.54.$

They were all capable of describing about 75 % of the observed variability for the calibration period (year 1, Table 2) and of reproducing observations equally well, where an apparent seasonal trend with maximum values of INPs₋₈ in summer is recognisable (Fig. 2, upper panel). Yet, model 1, based on two variables only – f_V and wind speed –, performed slightly better than the other two models, which are based on three parameters. It also provided the smallest maximum absolute error (Table 2). The range of potential concentrations of INPs₋₈ which can be predicted from model 1 is also the closest to observations. Inserting in the model the smallest, and largest, observed values of f_V and wind speed results in a range of calculated concentrations of 0.11 INPs₋₈ mL^{-1} , and 750 INPs₋₈ mL^{-1} . Doing the same with model 2 results in a maximum value of 250 INPs₋₈ mL^{-1} , and with model 3 of 400 INPs₋₈ mL^{-1} , underestimating the range of measured concentrations for at least one event. The observed rapid changes in the abundance of INPs₋₈ may explain the slightly better performance of model 1. Differences in the concentration of INPs₋₈ of more than 2 orders of magnitude were found not only on a seasonal timescale but also within the same precipitation event over a couple of hours. The variables “season” and, to a lesser extent, “source region”, “temperature”, and “ $\log(N_{>0.5} \text{ m}^{-3})$ ” could not always reproduce such sudden changes, as can be seen from the broader distribution of these parameters in Fig. 1.

The pattern of residuals over time is almost the same for all three models (Fig. 2, lower panel). Thus, it is unlikely to result from random noise and suggests the presence of at least one further driver of the abundance of INPs₋₈ in precipitation. Given the lack of any relationship with precipitation intensity, a likely candidate is the average mass (equivalent liquid volume) of hydrometeors formed by individual INPs. For snow crystals it spans over more than an order of magnitude (Mason, 1957). INPs generating larger hydrometeors, such as those grown through riming, will be diluted in a larger volume of water and result in an overestimation

Table 2. Summary of the main statistics employed to evaluate the quality of the models. “ R_{adj}^2 ” is the fraction of the observed variance reproduced by a model. It is adjusted to account for the number of variables and samples considered. All models, parameters, and constants are highly significant ($p < 0.001$), except the parameter “source region” ($p = 0.06$). “ β^* ” is the value of the standardised regression coefficients, expressing the relative importance of each parameter in a model. The “residuals” column shows the median residual value “med” and the maximum absolute residual as maximum estimation error “ABS” (the corresponding factors of error estimate on linear scale are shown in brackets). “MSE” is the value of the mean squared error.

	Calibration		Validation	
	R_{adj}^2	β^*	residuals	residuals
1	0.76	f_V : 0.62 wind speed: 0.47	Med: -0.04 (0.9) ABS: 1.02 (10.4) MSE: 0.16	Med: -0.08 (0.8) ABS: 0.87 (7.4) MSE: 0.25
2	0.73	season: 0.52 wind speed: 0.52 source region: 0.12	Med: 0.00 (1.0) ABS: 1.45 (28.4) MSE: 0.17	Med: -0.25 (0.6) ABS: 1.42 (26.1) MSE: 0.56
3	0.74	wind speed: 0.49 temperature: 0.48 $\log(N_{>0.5 \text{ m}^{-3}})$: 0.26	Med: -0.02 (0.9) ABS: 1.22 (16.5) MSE: 0.17	Med: -0.33 (0.5) ABS: 1.13 (13.5) MSE: 0.43

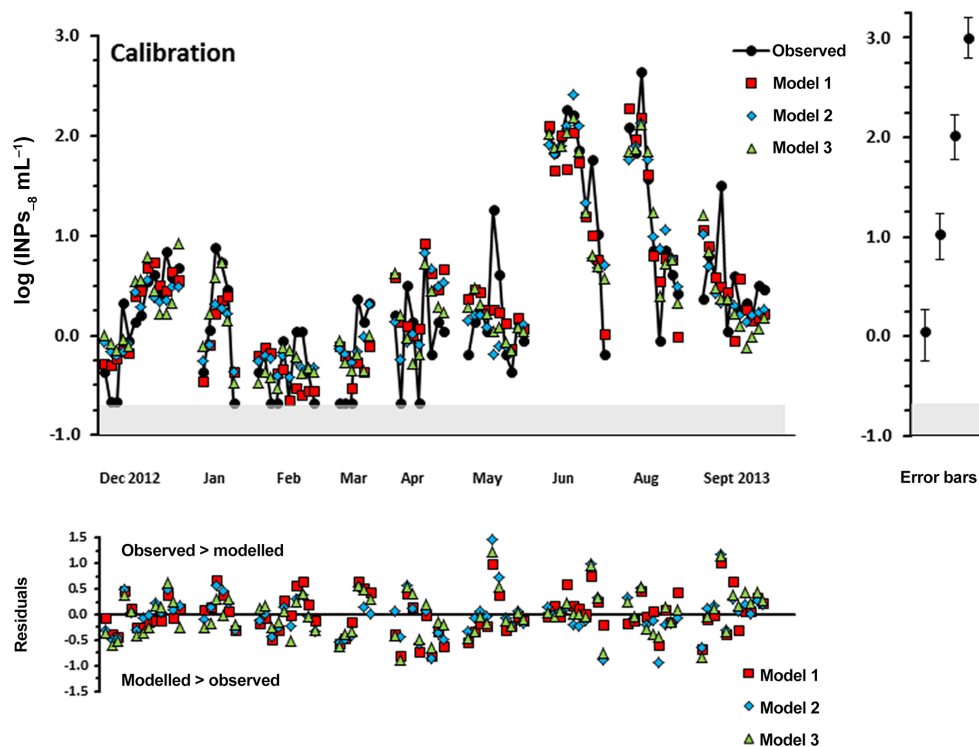


Figure 2. Comparison of observed concentrations of INPs_{-8} with the values predicted by models (absolute values in upper panels, residuals in lower panels) for the data set used for calibration ($n = 84$). The grey area in the upper panel indicates the range below the detection limit of our observation method. Time proceeds from left to right, intervals are not to scale, dots belonging to the same sampling campaign are connected by lines. Error bars associated to the measurement of 1, 10, 100, and 1000 $\text{INPs}_{-8} \text{ mL}^{-1}$ are represented close to the graph.

of modelled numbers of $\text{INPs}_{-8} \text{ mL}^{-1}$. Smaller than average ice crystals will do the opposite.

3.2 Model validation

We validated the three models with observations from 15 precipitation samples collected between May and October 2014. The values of the environmental parameters associated with these 15 independent samples (f_V , air temperature, etc.) were directly inserted in the equations of the three models as derived from the calibration step and used to predict values of $\text{INPs}_{-8} \text{ mL}^{-1}$.

The observed concentrations of INPs_{-8} during this second period of measurements ranged from 0.21 mL^{-1} to a maximum of 60 mL^{-1} . Interestingly, the samples collected in 2014 presented a completely different pattern compared to the previous year of observations (Fig. 1, green squares; Fig. 3, upper panel). The lowest concentrations of INPs_{-8} were observed during summer, whilst the highest concentrations occurred in May during a Saharan dust event and in October when a cold front from northern Europe reached Jungfraujoch (air temperature dropped to -16°C). For the sampling campaigns carried out in June, July, and September the local air temperature was relatively warm (between -7 and $+3^\circ\text{C}$). Still, f_V values were low, between 0.23 and 0.47, suggesting that air masses had already lost substantial parts of their initial water vapour prior to arrival at Jungfraujoch, even if season, source region, and local temperature could have been favourable for an abundant residual presence of INPs_{-8} .

As a consequence, models 2 and 3, which are based either on season, source region, or air temperature, predicted a smaller variability of INPs than observed and overestimated the low concentrations measured in summer 2014 causing larger residual values (Fig. 3 lower panel, Table 2). Model 1, based only on the two parameters f_V and wind speed, provided better results in predicting the variability of INPs_{-8} observed during the second year of sampling, producing lower absolute errors, less than 1 log unit (Table 2).

3.3 Source and sink effects

Even if the linear coefficients are site specific, the three models presented in this paper point at important general indications. Wind speed is a necessary parameter to describe INPs_{-8} in precipitation and is related to $N_{>0.5}$ and to a more recent land contact represented by the ratio NO_y / CO (Table 1). Other factors can be combined to wind speed obtaining models of comparable quality. These factors are f_V , temperature, season, source region, and $N_{>0.5}$ and are all well correlated among themselves (Table 1). This means that their relation with INPs_{-8} can be linked to the same process, which can be particle processing in precipitating clouds. This can act as a “sink” force for INPs_{-8} and is best represented by f_V . On the other hand, wind speed can strengthen

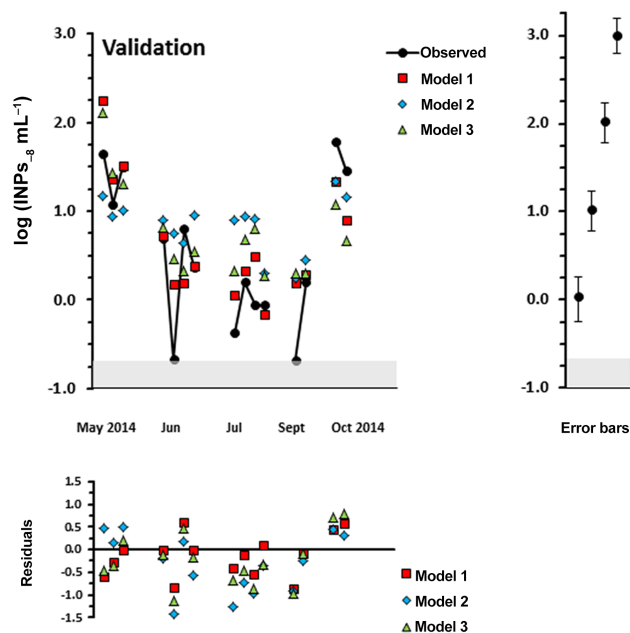


Figure 3. Comparison of observed concentrations of INPs_{-8} with the values predicted by models (absolute values in upper panels, residuals in lower panels) for the data set used for validation ($n = 15$). The grey area in the upper panel indicates the range below the detection limit of our observation method. Time proceeds from left to right, intervals are not to scale, dots belonging to the same sampling campaign are connected by lines. Error bars associated to the measurement of 1, 10, 100, and 1000 $\text{INPs}_{-8} \text{ mL}^{-1}$ are represented close to the graph.

the “source” of airborne particles. To different degrees, surfaces on Earth, such as oceans, forests, crops, soils, freshwaters, and snowpack, host organisms with ice nucleating activity (Després et al., 2012) and may contribute to the airborne population of INPs_{-8} . In this perspective, source region and seasonality may relate more to the likelihood for an air mass to reach Jungfraujoch with a lot of particles and little prior precipitation rather than to a different background number of airborne INPs_{-8} . Therefore, it is possible to imagine that, independent from a more or less constant and widespread reservoir of INPs_{-8} , it is the combination of the energy of an air mass with the amount of precipitation generated by this air mass that determines the residual abundance of INPs_{-8} in precipitation samples.

4 Conclusions

Large variability in the abundance of INPs_{-8} has been found in over a hundred precipitation samples collected at Jungfraujoch (3580 m a.s.l.), with values ranging from 0.21 to 434 $\text{INPs}_{-8} \text{ mL}^{-1}$. Strikingly, with simple multiple linear regression models based on some easily measurable environmental parameters it was possible to describe and predict up

to 75 % of the observed variability in INPs₋₈. All these models indicate that the variability of INPs₋₈ is determined by the interaction of “source” and “sink” processes, such as the potential for air masses to pick up and transport INPs₋₈ from several sources and for INPs₋₈ to be removed by precipitation. Our investigation indicates that a large abundance of INPs₋₈ in precipitation at Jungfraujoch is present whenever there is a coincidence of high wind speed and moist air mass with little or no prior precipitation. Based on the results of the present study, INPs active at moderate supercooling are expected to be abundant whenever high wind speed coincides with first (initial) precipitation from an air mass. These conditions can be met when an air mass is suddenly forced to rise, for instance at the boundary of a front or due to thermal updrafts or when crossing a mountain ridge. Specifically during the passage of a cold front, gusty winds promote the uptake of particles and the first clouds that form will still retain a large fraction of the initial water vapour of the warm air mass (Gayet et al., 2009; Wright et al., 2014). Simultaneously, physical conditions along a cold front are favourable for cloud formation. Therefore, frequent systematic coincidences of high numbers of INPs with meteorological conditions conducive to precipitation may be expected. Due to this frequent co-occurrence, the potential impact on precipitation by INPs active at slight supercooling – such as INPs of biological origin – may be larger than previously estimated. Their role in the water cycle might therefore best be studied under such conditions.

5 Data availability

The data set for this paper is publicly available as Supplement.

The Supplement related to this article is available online at doi:10.5194/acp-16-8341-2016-supplement.

Author contributions. Emiliano Stopelli and Franz Conen did the field measurements at Jungfraujoch on the concentrations of INPs, analysed data, did statistical modelling, and wrote the manuscript. Erik Herrmann, Stephan Henne, and Martin Steinbacher respectively, provided data and support for the interpretation of $N_{>0.5}$, FLEXPART modelling, PM₁₀ and trace gases and contributed to writing the paper. Cindy E. Morris and Christine Alewell provided strong conceptual frameworks and contributed to writing the paper. The authors declare no competing financial interests.

Acknowledgements. We thank the International Foundation for High Alpine Research Station Jungfraujoch and Gornergrat (HF-SJG) for making it possible for us to conduct our measurements

at Jungfraujoch. Urs and Maria Otz, and Martin and Joan Fischer provided helpful support during field activity. Corinne Baudinot measured the abundance of INPs in snow samples during the second year of observations. Dr Thomas Kuhn and Mark Rollog analysed the stable isotope ratio in our snow water samples. We thank MeteoSwiss for providing data on meteorology at Jungfraujoch. The work described here was supported by the Swiss National Science Foundation (SNF) through grant no. 200021_140228 and 200020_159194. Measurements of total solid particles were performed by Paul Scherrer Institute in the framework of the Global Atmospheric Watch (GAW) programme funded by MeteoSwiss with further support provided by the European FP7 project BACCHUS (grant agreement no. 603445). Trace gases and PM₁₀ measurements at Jungfraujoch are performed as part of the Swiss National Air Pollution Monitoring Network, which is operated by Empa in collaboration with the Swiss Federal Office for the Environment.

Edited by: T. Koop

Reviewed by: two anonymous referees

References

- Bowers, R. M., Lauber, C. L., Wiedinmyer, C., Hamady, M., Hallar, A. G., Fall, R., Knight, R., and Fierer, N.: Characterization of airborne microbial communities at a high-elevation site and their potential to act as atmospheric ice nuclei, *Appl. Environ. Microbiol.*, 75, 5121–5130, doi:10.1128/AEM.00447-09, 2009.
- Brunner, D., Henne, S., Keller, C. A., Vollmer, M. K., Reimann, S., and Buchmann, B.: Estimating European Halocarbon Emissions Using Lagrangian Backward Transport Modeling and in Situ Measurements at the Jungfraujoch High-Alpine Site, *Lagrangian Modeling of the Atmosphere*, edited by: Lin, J., Brunner, D., Gerbig, C., Stohl, A., Luhar, A., and Webley, P., American Geophysical Union, Washington DC, 207–221, doi:10.1029/2012GM001258, 2013.
- Cantrell, W. and Heymsfield, A.: Production of Ice in Tropospheric Clouds: A Review, *B. Am. Meteorol. Soc.*, 86, 795–807, doi:10.1175/BAMS-86-6-795, 2005.
- Christner, B. C., Cai, R., Morris, C. E., McCarter, K. S., Foreman, C. M., Skidmore, M. L., Montross, S. N., and Sands, D. C.: Geographic, seasonal, and precipitation chemistry influence on the abundance and activity of biological ice nucleators in rain and snow, *P. Natl. Acad. Sci. USA*, 105, 18854–18859, doi:10.1073/pnas.0809816105, 2008.
- Conen, F., Rodriguez, S., Hüglin, C., Henne, S., Herrmann, E., Bukowiecki, N., and Alewell, C.: Atmospheric ice nuclei at the high-altitude observatory Jungfraujoch, Switzerland, *Tellus B*, 67, 1–10, doi:10.3402/tellusb.v67.25014, 2015.
- Crawford, I., Bower, K. N., Choularton, T. W., Dearden, C., Crosier, J., Westbrook, C., Capes, G., Coe, H., Connolly, P. J., Dorsey, J. R., Gallagher, M. W., Williams, P., Trembath, J., Cui, Z., and Blyth, A.: Ice formation and development in aged, wintertime cumulus over the UK: observations and modelling, *Atmos. Chem. Phys.*, 12, 4963–4985, doi:10.5194/acp-12-4963-2012, 2012.
- Creamean, J. M., Suski, K. J., Rosenfeld, D., Cazorla, A., DeMott, P. J., Sullivan, R. C., White, A. B., Ralph, F. M., Minnis, P., Comstock, J. M., Tomlinson, J. M., and Prather, K. A.:

- Dust and biological aerosols from the Sahara and Asia influence precipitation in the western U.S., *Science*, 339, 1572–1578, doi:10.1126/science.1227279, 2013.
- DeMott, P. J., Prenni, A. J., Liu, X., Kreidenweis, S. M., Petters, M. D., Twohy, C. H., Richardson, M. S., Eidhammer, T., and Rogers, D. C.: Predicting global atmospheric ice nuclei distributions and their impacts on climate, *P. Natl. Acad. Sci. USA*, 107, 11217–11222, doi:10.1073/pnas.0910818107, 2010.
- Després, V. R., Huffman, J. A., Burrows, S. M., Hoose, C., Safatov, A. S., Buryak, G., Fröhlich-Nowoisky, J., Elbert, W., Andreae, M. O., Pöschl, U., and Jaenicke, R.: Primary biological aerosols particles in the atmosphere: a review, *Tellus B*, 64, 15598, doi:10.3402/tellusb.v64i0.15598, 2012.
- Fröhlich, R., Cubison, M. J., Slowik, J. G., Bukowiecki, N., Canonaco, F., Croteau, P. L., Gysel, M., Henne, S., Herrmann, E., Jayne, J. T., Steinbacher, M., Worsnop, D. R., Baltensperger, U., and Prévôt, A. S. H.: Fourteen months of on-line measurements of the non-refractory submicron aerosol at the Jungfraujoch (3580 m a.s.l.) – chemical composition, origins and organic aerosol sources, *Atmos. Chem. Phys.*, 15, 11373–11398, doi:10.5194/acp-15-11373-2015, 2015.
- Gayet, J. F., Treffeisen, R., Helbig, A., Bareiss, J., Matsuki, A., Herber, A., and Schwarzenboeck, A.: On the onset of the ice phase in boundary layer Arctic clouds, *J. Geophys. Res.*, 114, 1–15, doi:10.1029/2008JD011348, 2009.
- Griffiths, A. D., Conen, F., Weingartner, E., Zimmermann, L., Chambers, S. D., Williams, A. G., and Steinbacher, M.: Surface-to-mountaintop transport characterised by radon observations at the Jungfraujoch, *Atmos. Chem. Phys.*, 14, 12763–12779, doi:10.5194/acp-14-12763-2014, 2014.
- Hammer, Ø., Harper, D. A., and Ryan, P. D.: PAST: PALEontological STatistics software package for education and data analysis, *Palaeontol. Electron.*, 4, available at: http://www.uv.es/pe/2001_1/past/past.pdf (last access: 6 January 2016), 2001.
- Huffman, J. A., Prenni, A. J., DeMott, P. J., Pöhlker, C., Mason, R. H., Robinson, N. H., Fröhlich-Nowoisky, J., Tobo, Y., Després, V. R., Garcia, E., Gochis, D. J., Harris, E., Müller-Germann, I., Ruzene, C., Schmer, B., Sinha, B., Day, D. A., Andreae, M. O., Jimenez, J. L., Gallagher, M., Kreidenweis, S. M., Bertram, A. K., and Pöschl, U.: High concentrations of biological aerosol particles and ice nuclei during and after rain, *Atmos. Chem. Phys.*, 13, 6151–6164, doi:10.5194/acp-13-6151-2013, 2013.
- IAEA (International Atomic Energy Agency): Environmental isotopes in the hydrological cycle, Principles and applications, Vol. 2. Atmospheric Water, available at: http://www-naweb.iaea.org/naweb/ih/IHS_resources_publication_hydroCycle_en.html (last access: 6 January 2016), 2001.
- Jiang, H., Yin, Y., Yang, L., Yang, S., Su, H., and Chen, K.: The Characteristics of Atmospheric Ice Nuclei Measured at Different Altitudes in the Huangshan Mountains in the Southwest China, *Adv. Atmos. Sci.*, 31, 396–406, doi:10.1007/s00376-013-3048-5, 2014.
- Joly, M., Amato, P., Deguillaume, L., Monier, M., Hoose, C., and Delort, A.-M.: Quantification of ice nuclei active at near 0°C temperatures in low-altitude clouds at the Puy de Dôme atmospheric station, *Atmos. Chem. Phys.*, 14, 8185–8195, doi:10.5194/acp-14-8185-2014, 2014.
- Jones, A. M. and Harrison, R. M.: The effects of meteorological factors on atmospheric bioaerosol concentrations—a review, *Sci. Total Environ.*, 326, 151–180, doi:10.1016/j.scitotenv.2003.11.021, 2004.
- Kellogg, C. A. and Griffin, D. W.: Aerobiology and the global transport of desert dust, *Trends Ecol. Evol.*, 21, 638–644, doi:10.1016/j.tree.2006.07.004, 2006.
- Lindemann, J., Constantinidou, H. A., Barchet, W. R., and Upper, C. D.: Plants as sources of airborne bacteria, including ice nucleation-active bacteria, *Appl. Environ. Microb.*, 44, 1059–1063, 1982.
- Lindow, S. E., Army, D. C., and Upper, C. D.: Distribution of ice nucleation-active bacteria on plants in nature, *Appl. Environ. Microb.*, 36, 831–838, 1978.
- Mason, B. J.: *The Physics of Clouds*, Oxford University Press, 1957.
- Mason, B. J.: The rapid glaciation of slightly supercooled cumulus clouds, *Q. J. Roy. Meteor. Soc.*, 122, 357–365, doi:10.1002/qj.49712253003, 1996.
- Morris, C. E., Conen, F., Huffman, J. A., Phillips, V., Pöschl, U., and Sands, D. C.: Bioprecipitation: a feedback cycle linking earth history, ecosystem dynamics and land use through biological ice nucleators in the atmosphere, *Glob. Change Biol.*, 20, 341–351, doi:10.1111/gcb.12447, 2014.
- Mülmenstädt, J., Sourdeval, O., Delanoë, J., and Quaas, J.: Frequency of occurrence of rain from liquid-, mixed-, and ice-phase clouds derived from A-Train satellite retrievals, *Geophys. Res. Lett.*, 42, 6502–6509, doi:10.1002/2015GL064604, 2015.
- Murray, B. J., O’Sullivan, D., Atkinson, J. D., and Webb, M. E.: Ice nucleation by particles immersed in supercooled cloud droplets, *Chem. Soc. Rev.*, 41, 6519–6554, doi:10.1039/c2cs35200a, 2012.
- Pandey Deolal, S., Staehelin, J., Brunner, D., Cui, J., Steinbacher, M., Zellweger, C., Henne, S., and Vollmer, M. K.: Transport of PAN and NO_y from different source regions to the Swiss high alpine site Jungfraujoch, *Atmos. Environ.*, 64, 103–115, doi:10.1016/j.atmosenv.2012.08.021, 2013.
- Petters, M. D. and Wright, T. P.: Revisiting ice nucleation from precipitation samples, *Geophys. Res. Lett.*, 42, 8758–8766, doi:10.1002/2015GL065733, 2015.
- Pöschl, U., Martin, S. T., Sinha, B., Chen, Q., Gunthe, S. S., Huffman, J. A., Borrmann, S., Farmer, D. K., Garland, R. M., Helas, G., Jimenez, J. L., King, S. M., Manzi, A., Mikhailov, E., Pauliquevis, T., Petters, M. D., Prenni, A. J., Roldin, P., Rose, D., Schneider, J., Su, H., Zorn, S. R., Artaxo, P., and Andreae, M. O.: Rainforest Aerosols as Biogenic Nuclei of Clouds and Precipitation in the Amazon, *Science*, 329, 1513–1516, doi:10.1126/science.1191056, 2009.
- Prenni, A. J., Petters, M. D., Kreidenweis, S. M., Heald, C. L., Martin, S. T., Artaxo, P., Garland, R. M., Wollny, A. G., and Pöschl, U.: Relative roles of biogenic emissions and Saharan dust as ice nuclei in the Amazon basin, *Nat. Geosci.*, 2, 402–405, doi:10.1038/ngeo517, 2009.
- Prenni, A. J., Tobo, Y., Garcia, E., DeMott, P. J., Huffman, J. A., McCluskey, C. S., Kreidenweis, S. M., Prenni, J. E., Pöhlker, C., and Pöschl, U.: The impact of rain on ice nuclei populations at a forested site in Colorado, *Geophys. Res. Lett.*, 40, 227–231, doi:10.1029/2012GL053953, 2013.
- R Core Team: R: A Language and Environment for Statistical Computing, R Foundation for Statistical Computing, Vienna, Austria, 2016.

- tria, available at: <http://www.R-project.org> (last access: 6 January 2016), 2011.
- Stohl, A., Forster, C., Frank, A., Seibert, P., and Wotawa, G.: Technical note: The Lagrangian particle dispersion model FLEXPART version 6.2, *Atmos. Chem. Phys.*, 5, 2461–2474, doi:10.5194/acp-5-2461-2005, 2005.
- Stopelli, E., Conen, F., Zimmermann, L., Alewell, C., and Morris, C. E.: Freezing nucleation apparatus puts new slant on study of biological ice nucleators in precipitation, *Atmos. Meas. Tech.*, 7, 129–134, doi:10.5194/amt-7-129-2014, 2014.
- Stopelli, E., Conen, F., Morris, C. E., Herrmann, E., Bukowiecki, N., and Alewell, C.: Ice nucleation active particles are efficiently removed by precipitating clouds, *Sci. Rep.*, 5, 16433, doi:10.1038/srep16433, 2015.
- Weingartner, E., Nyeki, S., and Baltensperger, U.: Seasonal and diurnal variation of aerosol size distributions ($10 < D < 750$ nm) at a high-alpine site (Jungfraujoch 3580 m asl), *J. Geophys. Res.*, 104, 809–826, doi:10.1029/1999JD900170, 1999.
- WMO/GAW World Meteorological Organisation/ Global Atmospheric Watch: Aerosol Measurements Procedures, Guidelines and Recommendations, available at: <https://www.wmo.int/pages/prog/gcos/documents/gruanmanuals/GAW/gaw143.pdf> (last access: 6 January 2016), 2003.
- Wright, T. P., Hader, J. D., McMeeking, G. R., and Petters, M. D.: High Relative Humidity as a Trigger for Widespread Release of Ice Nuclei, *Aerosol Sci. Tech.*, 48, i–v, doi:10.1080/02786826.2014.968244, 2014.